

## AN EXPERIMENTAL STUDY OF FRETTING BY MEANS OF X-RAY DIFFRACTION

G. H. FARRAHI† and G. MAEDER‡

Ecole Nationale Supérieure d'Arts et Métiers (ENSAM) 151, Bd de l'Hôpital, 75013 Paris, France

(Received 8 March 1991)

**Abstract**—This paper introduces a new method of investigation in the field of fretting. This method employs X-ray diffraction for the characterization of surface layer damage through residual stresses and work-hardening by tribological action. The effect of hardness and material residual stresses upon the state of the surface have been studied. The results showed that fretting, being a surface phenomenon, created work-hardening of soft material or work-softening of hard material in the near-surface layers. When the initial residual stresses were high, fretting could not modify them because they had already reached the saturation limit. A Pole figure shows that fretting modified the texture of the specimen surface.

### INTRODUCTION

The mechanical and chemical state of a surface have an important role in tribological phenomenon and may be characterized by a number of parameters, including:

- (i) micro-geometry (surface roughness)
- (ii) physico-chemical nature of the surface.
- (iii) mechanical characteristics (hardness, work-hardening, residual stresses...) of the surface.

With the exception of hardness this last aspect has rarely been taken into account. This is because of the difficulties in measuring and calculating the residual stresses and plastic deformation present in the material. One of the methods allowing us to determine these mechanical parameters is the X-ray diffraction technique. This method being non-destructive makes it possible to study the surface layers of 5–100  $\mu\text{m}$  dependent on the material and the nature of the employed X-ray tube.

Fretting being a surface damage event occurs between contacting surfaces which are subjected to vibration or cyclic stressing. It arises, for instance, in shrink fits, press fits, bolted assemblies, keyed gears and even between electrical contacts.

The X-ray technique has been used for research into sliding [1, 2] and rolling contact [3]. A similar investigation by the authors [4] showed that X-ray diffraction can be used to study fretting phenomena. It was shown that the residual stresses introduced by fretting were compressive and had their maximum value on the surface. The residual stresses perpendicular to the fretting direction  $\sigma_{22}$  were larger than those in the direction of fretting  $\sigma_{11}$  [4]; see for example Fig. 1.

†Present address: Department of Mechanical Engineering, University of Sheffield, Mappin Street, Sheffield S1 3JD, England.

‡Present address: Direction de la Recherche, Renault, 9-11 Ave 18 juin 1940, 92500 Rueil-Malmaison, France.

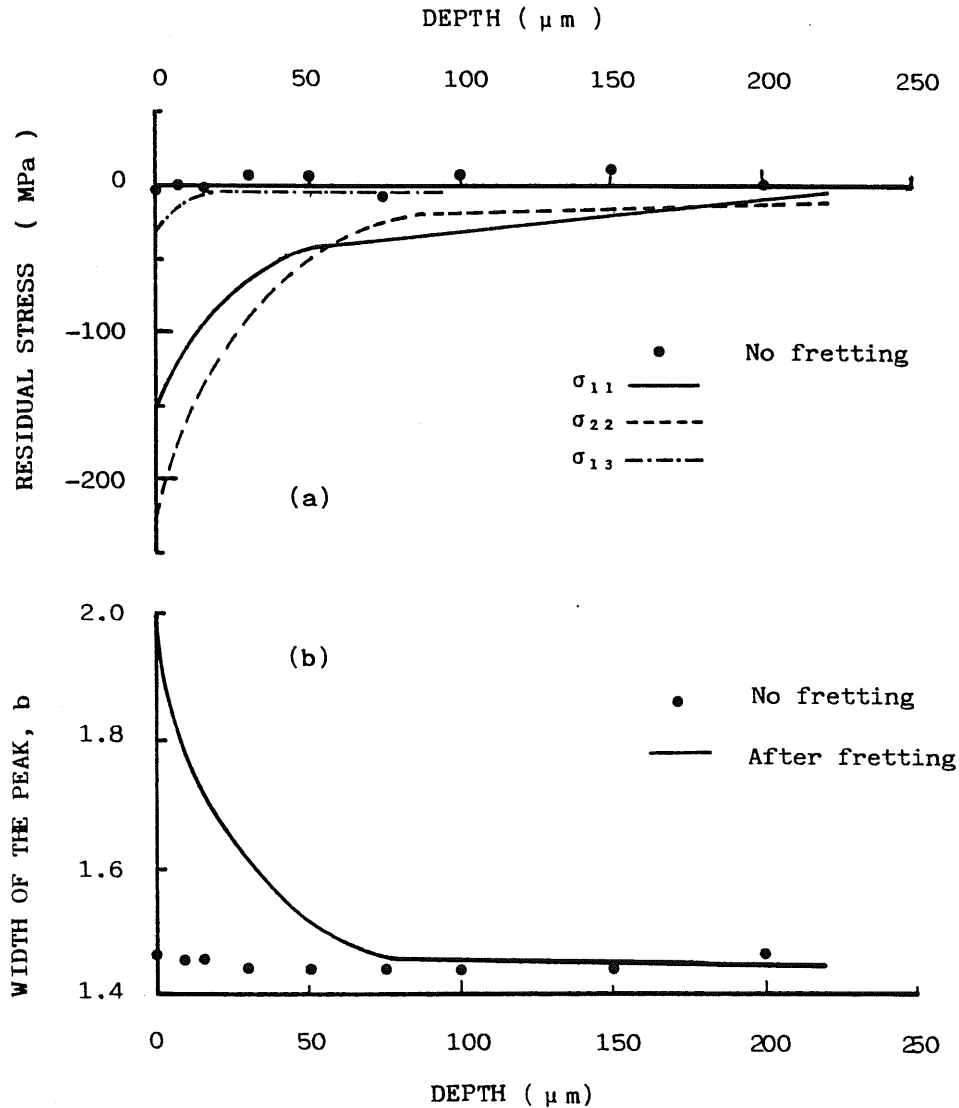


Fig. 1. Typical results of the effect of fretting due to a normal load of 360 N and stressing at 50 Hz (after [4]). (a) Residual stresses and (b) the width of the diffraction peak characterizing the micro-strain before and after fretting.

### EXPERIMENTAL DETAILS

Figure 2 shows the fretting test machine. Movement is generated by a motor of variable speed. The rotational movement is transformed to a cyclic translatory movement by an eccentric whose vertical position is adjustable. The movement is then transmitted to the upper specimen holder by some articulations consisting of flexible plates of spring steel. Specimens are gripped in two specimen holders. The lower specimen holder is set up on the chassis via a double universal joint ensuring perfect alignment and consequently a good contact between the two specimens. The contact force is applied by a bolt through a coil spring and measured by a piezoelectric transducer. Slip amplitude is measured by an Eddy-current non-contacting transducer. Other measured parameters are: the frequency of fretting, the number of cycles and the electrical resistance of the contact. The slip amplitude (peak-to-peak) of this machine can vary from 0 to 75  $\mu\text{m}$ . The maximum normal load which can be applied is 1 kN. The machine can operate at frequencies in the range 2–70 Hz.

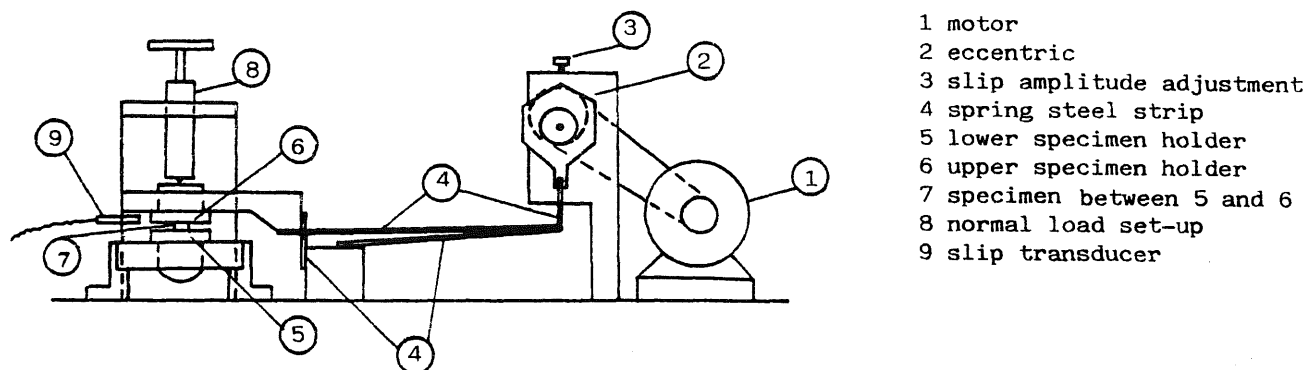


Fig. 2. Fretting test machine.

Fretting experiments were performed on an AFNOR XC48 steel of composition (wt%) 0.49 C, 0.73 Mn, 0.18 Si remainder Fe, and an AFNOR 35NCD16 steel of composition (wt%) 0.36 C, 0.4 Mn, 0.36 Si, 3.85 Ni, 1.75 Cr, 0.4 Mo remainder Fe. Table 1 shows the mechanical properties of these two steels which we employed in the first series of our investigation concerned with the influence of material hardness. The second series of tests concerned with the influence of initial residual stress was carried out only on 35NCD16 material. Specimens from 35NCD16 were cut and quenched in oil with one set of specimens being tempered at 873 K for 1 h, in a vacuum furnace, after having been ground. Another set of specimens was ground after having been tempered at the same temperature and for the same duration of time as that of the first set. The surface roughness of the two sets of specimens was identical. A pair of specimens in any one test was of the same material and treated identically. The contact configuration was flat-on-flat. The shape and dimensions of the test specimens are shown in Fig. 3. The linear oscillatory motion of fretting in our test followed the direction of the initial grinding of the specimens. The tests were carried out in the ambient air of the laboratory with an average humidity of 50% and an average temperature of 293 K. The fretting slip amplitude for all tests was  $55 \mu\text{m}$  (peak-to-peak). We applied a normal load of 360 N. Tests were carried out at a frequency of 50 Hz.

### RESIDUAL STRESSES AND X-RAY DIFFRACTION

The X-ray method measures strains in the surface layers of a material. These strains are then converted into stresses using various assumptions. The basic principle of obtaining the strain is simple [5, 6]. The interplanar spacing of a specific form of planes is obtained from grains of different orientations to the surface normal. This is determined by tilting and rotating the specimen with respect to the incident beam. This spacing is then converted into strains using the formula:

$$\varepsilon_{\phi\psi} = (d_{\phi\psi} - d_o)/d_o \quad (1)$$

Table 1. Mechanical properties of specimens

Material		0.2% Proof stress (MPa)	Hardness VHN
XC48	Annealed	379	192/5
	Quenched	1462	680/20
35 NCD16 quenched	Tempered at 600°C	1029	365/10
	Tempered at 200°C	1326	580/20

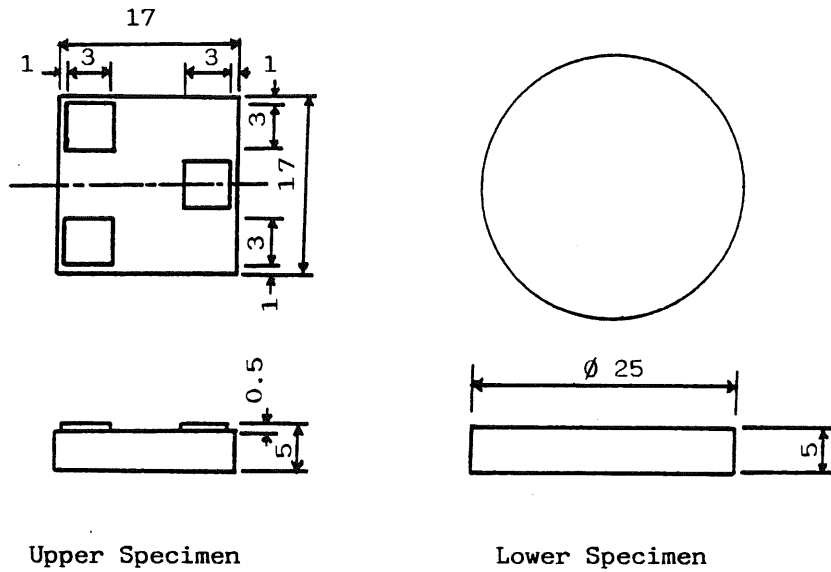


Fig. 3. Shape of the test specimens; dimensions in mm.

where  $d_0$  is the interplanar spacing for a stress free material, and  $d_{\phi\psi}$  is the spacing in the direction  $\phi\psi$ , defined by the angles  $\phi$  and  $\psi$  (Fig. 4). The spacing  $d_{\phi\psi}$  in equation (1) is obtained from the angular value of the Bragg peak corresponding to the diffraction planes using the formula:

$$2d \sin\Theta = \lambda \tag{2}$$

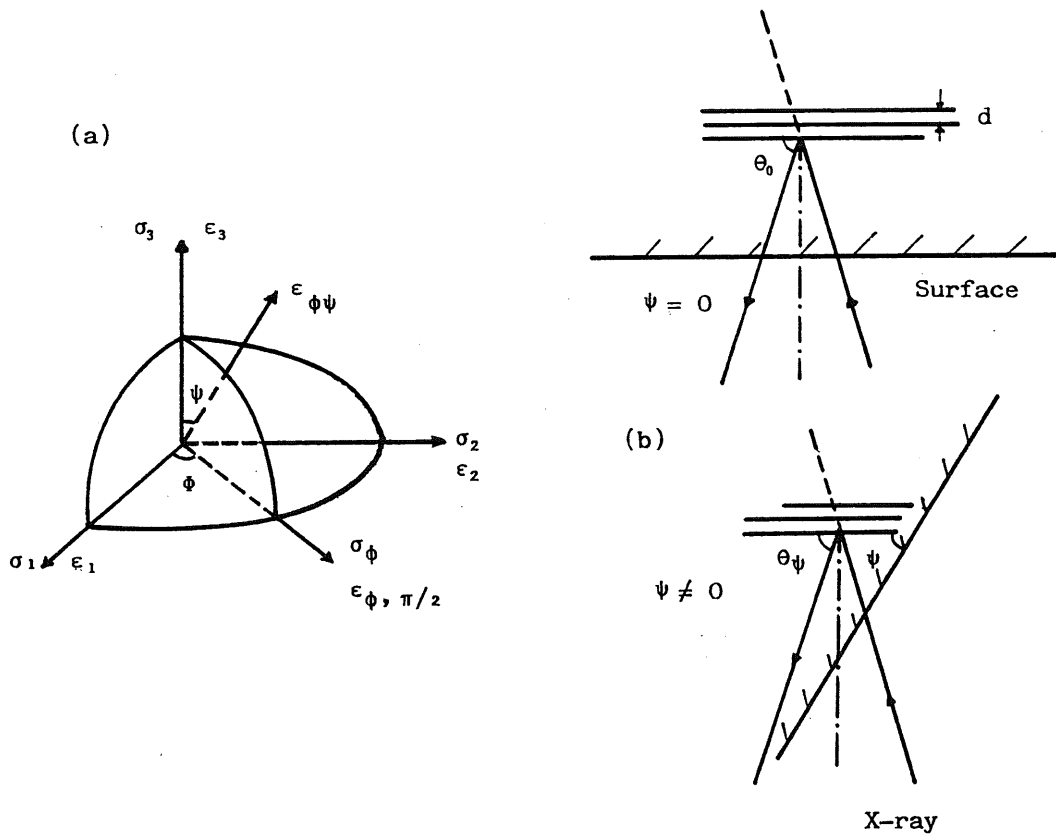


Fig. 4. Definition of parameters. (a) Definition of  $\phi$  and  $\psi$  and (b) orientation of planes to the surface.

where  $\lambda$  is the wavelength of the radiation. Differentiating Bragg's equation and substituting into equation (1) gives

$$\varepsilon = -1/2(\cot\theta)\Delta 2\theta \quad (3)$$

with  $\Delta 2\theta = 2\theta - 2\theta_0$ , where  $\theta_0$  is the angular position of the diffraction for a stress-free material. The strain  $\varepsilon_{\phi\psi}$  in the direction  $\phi\psi$  can be related to the stress  $\sigma$  by:

$$\varepsilon_{\phi\psi} = [(1 + \nu)/E]\sigma_{\phi} \cdot \sin^2\psi \quad (4)$$

where  $E$  is Young's modulus and  $\nu$  is Poisson's ratio for the material. Substituting equation (4) into equation (3) results in

$$\Delta 2\theta = -[(360/\pi)\tan\theta]\{[(1 + \nu)/E]\sigma_{\phi} \sin^2\psi\} \quad (5)$$

where  $(1 + \nu)/E = 1/2 S_2$  is the X-ray elastic constant which depends on the material and the orientation of the diffracting planes. By measuring the value of  $2\theta$  at different incident angles  $\phi$ , a linear relationship is found (for an isotropic material) of  $\Delta 2\theta$  against  $\sin^2\psi$ . The slope gives the value of the stress  $\sigma_{\phi}$ . The measurement of  $\varepsilon_{\phi\psi}$  for at least three directions of  $\phi$  together with the 3D-stress-strain relationship enables us to obtain the stress tensor. The broadening of the diffraction peak can be analysed in terms of micro-strain (Fig. 5). We measured the width of the diffraction line at 0.4 of the height,  $b$ , of the diffraction peak and this parameter may be used to characterize the micro-strain.

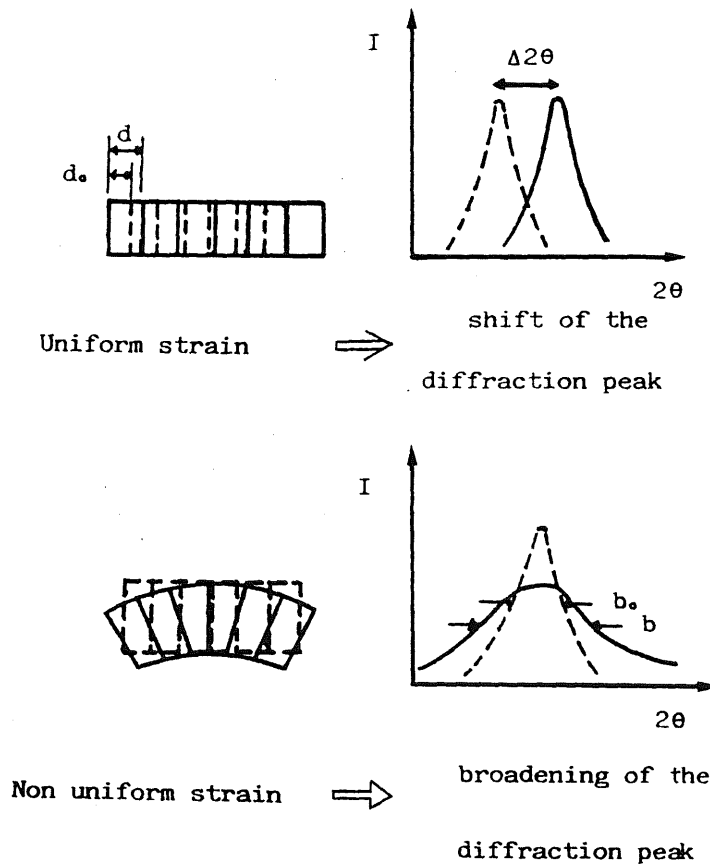
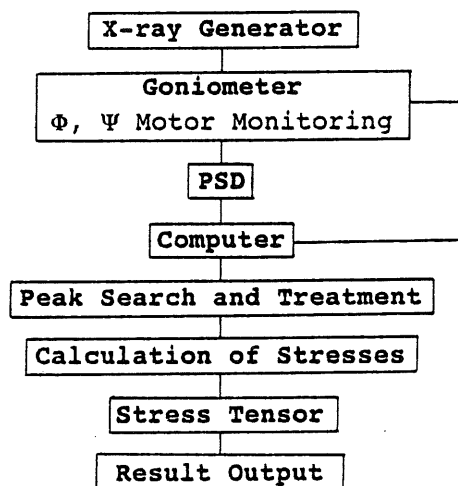


Fig. 5. Shift and broadening of an X-ray diffraction peak.

Table 2. Flow chart of X-ray measurements



The procedure for residual stress measurement is simple. The beam generated in an X-ray tube is focused and directed to the specimen, which is arranged in the centre of a goniometer. The X-rays are diffracted by favourably situated lattice planes and this produces interference. A detector is used to find the location and intensity of the diffracted beam. A computer is employed for monitoring the operation, collecting and analysing the data; see Table 2.

In our experiments a diffractometer equipped with an  $\Omega$  type goniometer (CGR/GS 2000), a position sensitive detector (PSD) and pulse height analyzer (INEL) were employed. A PDP 11/23 computer was used for monitoring and analysing the data. Chromium radiation ( $\lambda_{K\alpha} = 0.22895$  nm; 25 kV, 22 mA) was employed to examine the  $\{211\}$  peak ( $2\theta = 156^\circ$ ). The irradiated spot on a specimen was  $\Phi$  2 mm. For each stress-tensor 50 peaks ( $5 \phi$  angles by  $10 \psi$  angles) were examined. The X-ray elastic constant employed in the data analysis was measured and it was as follows:

$$1/2 S_2\{211\} = 5.8 \times 10^{-6} \text{ MPa}^{-1}.$$

Back-reflection Debye-Scherrer rings were examined on films with chromium radiation. These rings were uniform, indicating good conditions of diffraction for the specimens.

In order to determine the stress distribution by depth, the surface layer of specimens was removed by electrolytic polishing.

## RESULTS AND DISCUSSION

The reproducibility and accuracy of our X-ray measurement and fretting tests have already been checked elsewhere [4]. The effect of the number of fretting cycles, slip amplitude and normal load has also been studied [4]. Below we show the influence of material hardness and the initial stress state on the residual stress developments and  $b$  the width of the diffraction line.

### *Hardness of material*

The intensity of residual stresses on a surface, due to fretting, is related to hardness, and therefore to the yield strength of the material. The harder the material the higher the residual stress on the surface and the thinner the affected layer. Regarding the micro-strain as detected by parameter  $b$ , fretting caused an increase of  $b$  in soft material. This increase is due to work-hardening of the

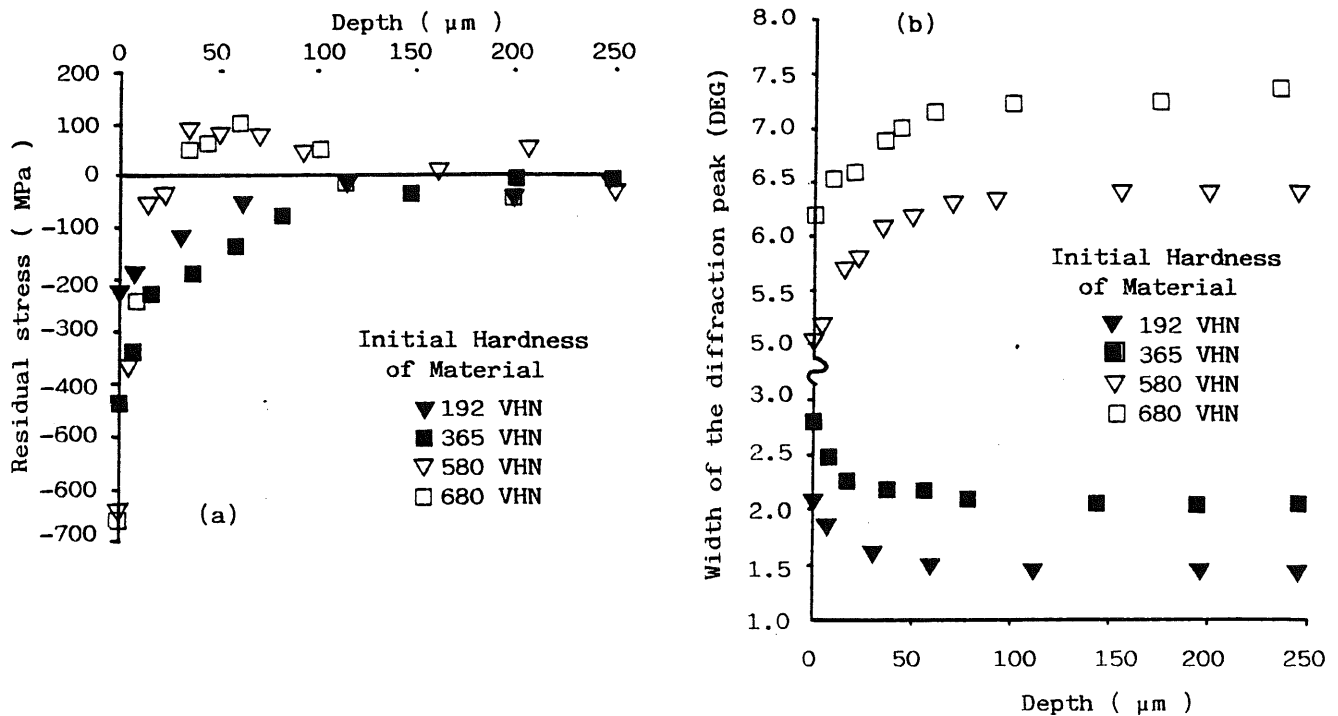


Fig. 6. Effect of the hardness upon (a) the residual stresses and (b) the width of the diffraction peak for two materials (slip amplitude  $55 \mu\text{m}$ ; frequency 50 Hz; number of fretting cycles  $5 \times 10^5$ ; normal load 360 N).

surface. On the other hand, fretting produced a decrease in  $b$  for initially hard material (Fig. 6). This decrease may be due to a dynamic recovery of the initial martensitic structure containing a high density of dislocations. The value of  $b$  can be related to the hardness: Kurita and Hirayama [6] and one of the authors [7] have already shown that the hardness of steel can be estimated by determining the width of the X-ray diffraction peak,  $b$ . Therefore an increase or a decrease of the width of the X-ray diffraction peak can be respectively interpreted as an increase or a decrease of hardness. By measuring the surface hardness, Waterhouse [8] has found that work-hardening or work-softening may occur because of fretting. It has been seen that fatigue [9] and shot peening [10] could cause a decrease of  $b$  in hard materials. It has been observed that cyclic stressing produces an increase in hardness on annealed material and a decrease on cold-drawn material. This change of hardness was dependent on both the magnitude of the cyclic stresses and the number of applied cycles. Miller [11] has shown that cyclic softening and cyclic hardening is strain rate dependent (i.e. frequency dependent). Smith *et al.* [12] studied a wide range of material and found that when the ratio of the ultimate tensile strength to the 0.2% proof stress is greater than 1.4 the material cyclically hardens, and when this ratio is less than 1.2 the material cyclically softens. For ratios between 1.2 and 1.4 it is difficult to predict cyclic changes.

#### Initial stress state

As we have already explained, this part of our investigation was carried out on two sets of specimens; one carrying an initial stress (ground) and another being tempered at  $600^\circ\text{C}$  and therefore devoid of residual stress. The measurement of residual stresses and parameter  $b$  on a ground specimen showed that grinding created similar stresses to those produced by fretting. This means that residual stresses created by grinding were compressive and they had their largest values on the surface. They were highest in the direction perpendicular to that of grinding, i.e. in the direction of  $\sigma_{22}$ . As Fig. 7 shows fretting could not alter greatly the distribution of residual stresses

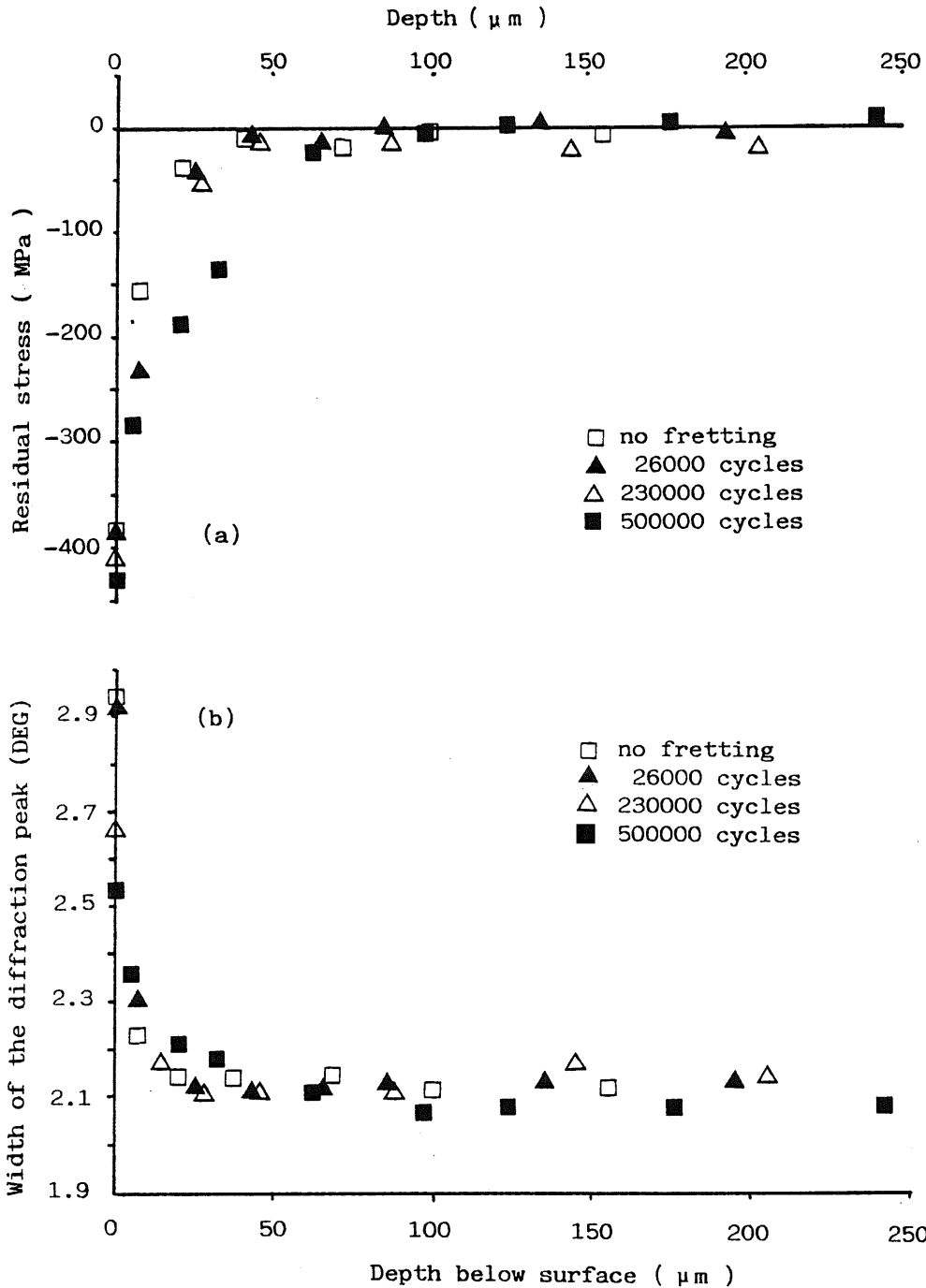


Fig. 7. Influence of the number of fretting cycles on the distribution of (a) the residual stresses and (b) the width of the diffraction peak on a ground specimen (35 NCD 16; hardness  $365 H_v$ ; slip amplitude  $55 \mu\text{m}$ ; frequency 50 Hz; normal load 360 N,  $\sigma_i = 0$ ).

already created by grinding. Nevertheless the width of the diffraction line, on the surface, decreased with increasing number of fretting cycles. This decrease, depending on the intensity of work-hardening introduced by grinding, may be due to a dynamic rearrangement of dislocations due to the fretting action. Figure 8 shows that residual stresses and parameter  $b$  increased by increasing the number of cycles when the specimen is devoid of any initial residual stress. Figure 9 provides a comparison of measured values of  $\sigma_{22}$  and  $b$  on the two sets of specimens. We observed that when



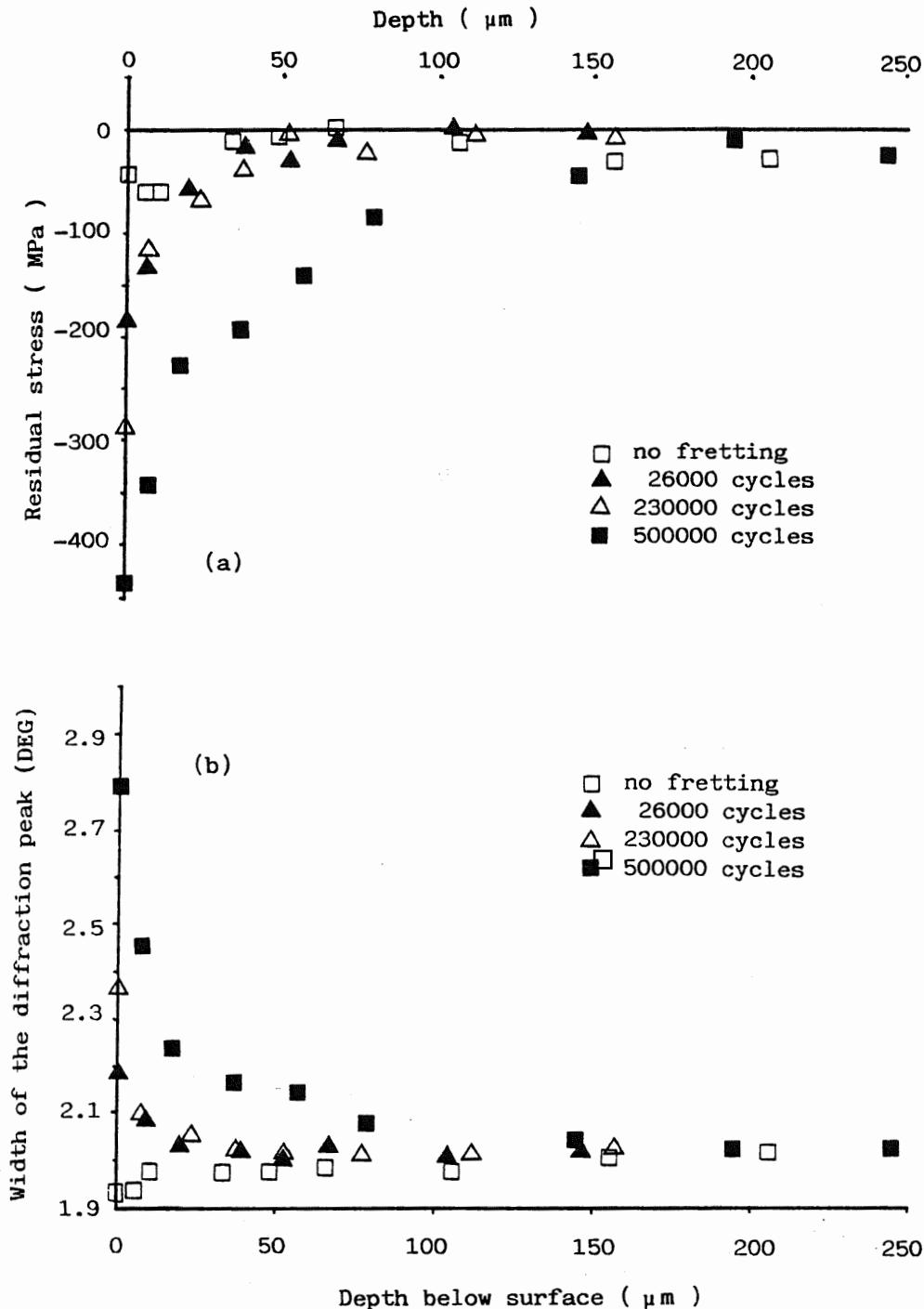


Fig. 8. Influence of the number of fretting cycles on the distribution of (a) the residual stresses and (b) the width of the diffraction peak on a tempered specimen (35 NCD 16; hardness  $365 H_v$ ; slip amplitude  $55 \mu\text{m}$ ; frequency 50 Hz; normal load 360 N,  $\sigma_i = 0$ ).

the residual stresses on a surface were sufficiently high, fretting could modify them only if the intensity and duration of the test were sufficient. However this was possible only when the residual stress had not reached the saturation limit which depends on the cyclic yield stress of the material. For both sets of specimens having different initial stress states we noticed that the value of  $\sigma_{22}$  (and also  $\sigma_{11}$ ) remained constant after  $5 \times 10^5$  cycles of fretting.

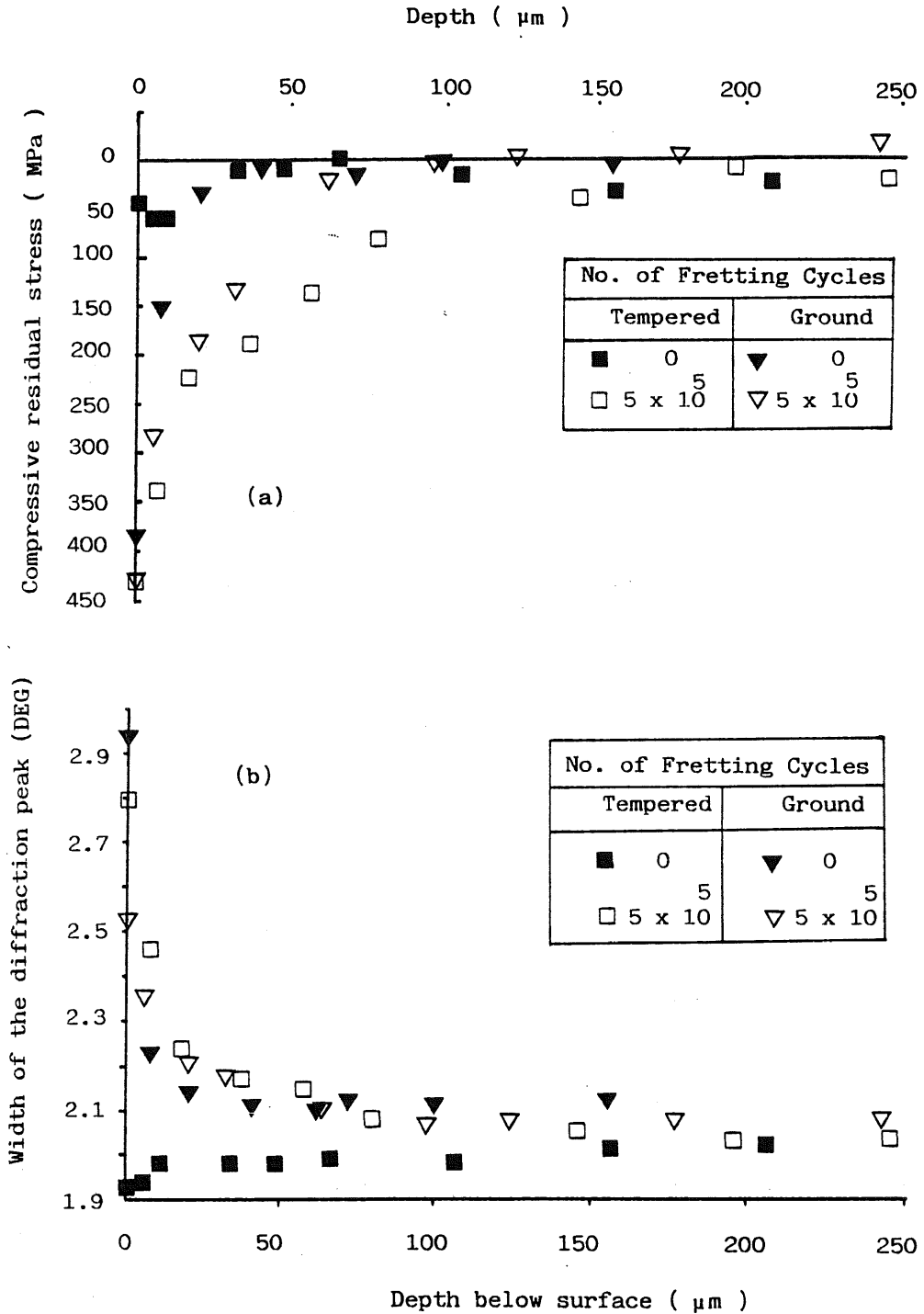


Fig. 9. Influence of the initial stresses on the distribution of (a) residual stresses and (b) the width of the diffraction peak (35 NCD 16; hardness  $365 H_v$ ; slip amplitude  $55 \mu\text{m}$ ; frequency 50 Hz; normal load 360 N).

### *Changes in crystallographic texture*

Since the properties of crystals are directionally dependent, the crystallographic orientation of the crystallites within the polycrystalline aggregate (i.e. texture) plays an important role. Texture may be the consequence of mechanical and/or heat treatments. The Pole figure is a common method for representing the texture. The Pole figure represents the orientation distribution function which

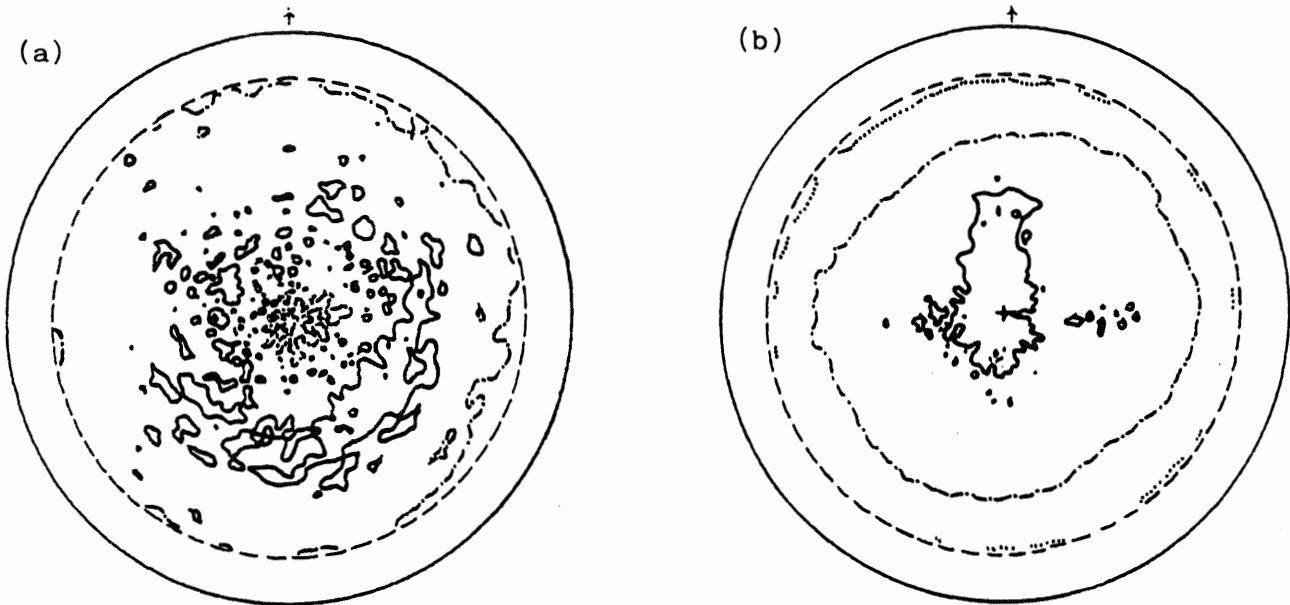


Fig. 10. Pole figure  $\{110\}$ . (XC48 annealed; hardness  $192 H_v$ ; slip amplitude  $55 \mu\text{m}$ ; frequency 50 Hz; normal load 360 N;  $5 \times 10^5$  cycles).

is not directly measurable. However the calculation of the orientation distribution from the Pole figure requires mathematical and computational analysis [13]. Analyses of the surfaces of contacting bodies during sliding [14] or rolling contact [15] has showed the development of textures; the intensity and magnitude of which changes during a test.

The Pole figure of the initial surface of a specimen from annealed XC48 (Fig. 10) shows the absence of any preferential orientation before fretting because of a negligible variation in intensity and a random distribution. The subsequent fretting motion led to the formation of a  $\{110\}$  texture parallel to the surface of the specimen. This has already been confirmed in the case of rolling contact experiments [15].

### CONCLUSIONS

From this work the following conclusions may be made.

- (1) Compressive residual stresses are introduced by fretting and attain a maximum value on the surface. The magnitude of this maximum depends on the yield strength of the material.
- (2) Work-hardening of soft materials and work-softening of hard materials can occur because of fretting.
- (3) When initial residual stresses on the contacting surfaces were high, fretting could modify them if the intensity and duration of the test were high enough. This occurs only when the residual stress has not reached a limiting value dependent on the cyclic yield strength.
- (4) Fretting modified the surface texture of the test pieces.

*Acknowledgement*—The authors would like to thank Dr J. L. Lebrun of ENSAM for his interest and helpful suggestions during this investigation.

### REFERENCES

1. J. W. Ho, C. Noyan and J. B. Cohen (1983) Residual stresses and sliding wear. *Wear* **84**, 183–202.
2. S. I. Nagashima and N. Tanaka (1983) A study of plastic flow and residual stress distribution caused by rolling contact. *Adv. X-ray Anal.* **27**, 207–212.

3. J. J. Wert, S. A. Singerman, R. A. Quarles and D. K. Chanhari (1984) An X-ray diffraction analysis of residual stresses induced by sliding wear of copper aluminium alloys. *JTEVA* **12**, 20–26.
4. G. H. Farrahi, P. H. Markho and G. Maeder (1991) A study of fretting wear with particular reference to measurement of residual stresses by X-ray diffraction. *Wear* **148**, 249–260.
5. G. Maeder (1986) X-ray diffraction and stress measurement. *Chem. Scr.* **26A**, 235–247.
6. M. Kurita and H. Hirayama (1984) An estimation of hardness of hardened steel by X-ray diffraction using a Gaussian curve fitting method. *JTEVA* **12**, 13–19.
7. G. H. Farrahi (1992) A non-destructive method of surface hardness measurement by X-ray diffraction. To be published.
8. R. B. Waterhouse (1972) *Fretting Corrosion*, pp. 102–104. Pergamon Press, Oxford.
9. H. Takechi, K. Namba, K. Rujiwara and K. Kawasaki (1981). Evaluation of subsurface fatigue damage in strip mill rolls by an X-ray diffraction method. *Trans. ISIJ* **21**, 92–99.
10. D. Hakimi (1984) Characterisation mecanique et metallurgique de la structure d'une couche grenaillee. Doct. 3eme Cycle thesis, University of Paris-sud, France.
11. K. J. Miller (1970) Cyclic behavior of materials. *J. Strain Anal.* **5**, 185–192.
12. R. W. Smith, M. H. Hirschberg and S. S. Manson (1963) Fatigue behaviour of materials under strain cycling in low and intermediate life range. NASA Tech. Note d-1574.
13. H. J. Bunge (1982) *Texture Analysis in Material Science*. Butterworths, London.
14. H. Krause and H. Ocalan (1984) The effect of initial orientation on the formation of tribological textures and on the wear behavior of the regions in the proximity of surface layers under continuous sliding motion in tribological systems. In *7th Int. Conf. on Texture of Materials* (Edited by C. M. Brakman, P. Jongenburger and E. J. Mittemijer), pp. 631–636. Icotom, The Netherlands.
15. H. Krause (1984) Development of tribological textures and residual stresses at the surface of contacting bodies during rolling/sliding motion. In *7th Int. Conf. on Texture of Materials* (Edited by C. M. Brakman, P. Jongenburger and E. J. Mittemijer), pp. 625–630. Icotom, The Netherlands.